A Statistical Method for Peak Localization in Hough Space by Analysing Butterflies

Zezhong Xu[1,2] and Bok-Suk Shin[1]

[1] Department of Computer Science, The University of Auckland
Auckland, New Zealand
[2] College of Computer Information Engineering, Changzhou Institute of Technology
Changzhou, Jiangsu, China
zxu531@aucklanduni.ac.nz, b.shin@auckland.ac.nz

Abstract. The Hough transform is an efficient method for extracting lines in images. Precision of detection relies on how to find and locate accurately the peak in Hough space after the voting process. In this paper, a statistical method is proposed to improve peak localization by considering quantization error and image noise, and by considering the coordinate origin selection. The proposed peak localization is based on butterfly analysis: statistical standard variances and statistical means are computed and used as parameters of fitting and interpolation processes. We show that accurate peak parameters are achieved. Experimental results compare our results with those provided by other peak detection methods. In summary, we show that the proposed peak localization method for the Hough transform is both accurate and robust in the presence of quantization error and image noise.

Keywords: Hough transform, peak detection, mean, variance.

1 Introduction

The *Hough transform* (HT) [5,11] is an efficient method for extracting geometric features in an image containing noisy, missing, and extraneous data. However, without further considerations, the HT requires a heavy computational load. In order to improve its efficiency, many proposals have been published, such as *fast HT* [16], *adaptive HT* [12], or special architectures [1] aiming at reducing the amount of computation and storage for real-time implementations. The *probabilistic HT* [15] and the *randomized HT* [24] only use selected sampling pixels for voting in the Hough space (also known as *accumulator array*). In addition, image noise and parameter quantization cause peak spreading in the Hough space.

Numerous methods are focused on peak enhancement in the accumulator array; the emphasis is here on generated distinct peaks and finding of those peaks. By modifying the HT voting scheme, peaks in the accumulator array are enhanced, and peak detection becomes easier. Edge information [3,9,17] and image preprocessing techniques [7,10,20] are used to guide the voting process.

R. Klette, M. Rivera, and S. Satoh (Eds.): PSIVT 2013, LNCS 8333, pp. 111–123, 2014.

By assigning different weights to votes, peaks becomes more distinct and peak finding becomes easier.

After finding a peak, there are two kinds of common methods to compute accurate peak parameters: simply select the absolute peak cell (θ,ρ) as potential solution, or take a weighted average [14,22] also including adjacent cells (θ_i,ρ_i). Two alternative accurate peak localization methods are presented in [18,19], where two different smoothing windows are employed. Weighted averaging is used to compute the θ value, and linear interpolation for the ρ value.

Recently, the *butterfly distribution* [8] in the accumulator array attracted attention. Several methods are motivated by the butterfly shape of a peak in Hough space. The butterfly shape was used for complete line segment detection in [2,4,23]. By analysing a butterfly pattern, the parameters of a line segment are extracted from the *butterfly's characteristics*; a local operator method [13] for peak enhancement proves to be more robust to image noise.

This paper proposes a novel statistical method for locating peaks in Hough space. The image centre is selected as the coordinates origin. After voting, the cell distribution is analysed around a peak in Hough space. By considering image noise and quantization error, the statistical mean and standard variance are computed and used to estimate a peak's parameters. An accurate peak is finally computed by fitting and interpolation.

The rest of the paper is organized as follows. Section 2 introduces an analysis of peak distribution in Hough space. Section 3 describes our peak finding and peak localization method based on statistical mean and variance. Section 4 compares by providing experimental results. Section 5 concludes.

2 Analysis of Peak Distribution

After voting, distribution of cells with voting values around a peak in Hough space resemble the shape of a butterfly. See Fig. 1. Those *butterfly patterns* (*butterflies* for short) have been analysed widely [8] in terms of shape and direction, also for understanding the width and length of the corresponding line segment.

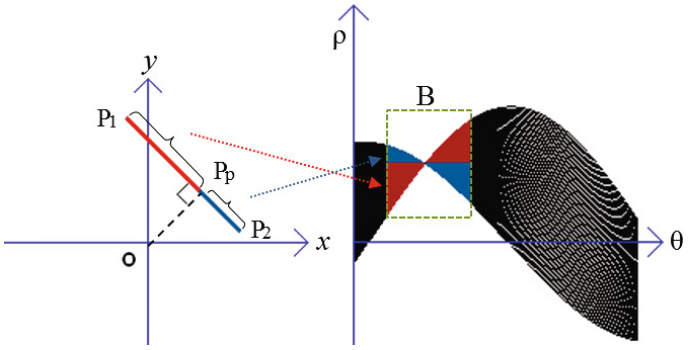

Fig. 1. Pixel contributions to cells. *Left*: Image space. *Right*: Hough space.

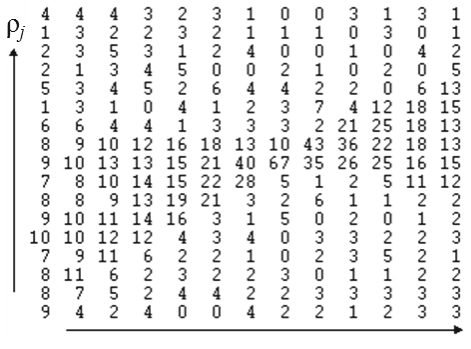

Fig. 2. Voting values for a noisy line segment in an image, with a peak at value 67

The technique presented in this paper is based on analysing the statistical structure of a butterfly.

Hough Space. A pixel in image space votes for many cells in Hough space. Let H_{ij} be the voting value at cell (i, j) in Hough space, i.e. at $\theta = i$ and $\rho = j$, where i and j are increments along ρ and θ coordinates. A *peak* at a cell (i, j) is formed by having a set of approximately collinear pixels voting for the same cell. See Fig. 2.

Although collinear pixels all contribute to the same peak, different pixels on a line also contribute to different parts around a peak in Hough space. Figure 1 illustrates that pixels left of the perpendicular point P_P contribute to the left-bottom part and the right-upper part from the peak in the butterfly region B. Pixels right of the perpendicular point P_P contribute to the left-upper part and the right-bottom part from the peak in the butterfly region B.

Butterfly Distribution around a Peak. When mapping one noise-free and zero-thickness line segment into Hough space with infinitesimal quantization, an *ideal butterfly* is produced which has two wings. The two wings are symmetrical and connect at the *symmetric point* or *peak* $(\theta_{peak}, \rho_{peak}) = \lambda$. Within an ideal butterfly, the sum $\sum_j H_{ij}$, i.e. for a variation in ρ-coordinates, remains identical, but the value of cell is changed in the same sum $\sum_j H_{ij}$. A program for analysing the Hough space needs to detect the symmetric point.

However, in the presence of image and quantization noise, *valid* (i.e. generated by the corresponding noisy line segment) voting values around a peak do not form an ideal symmetric point. For every column around a peak, sums of valid values in cells are only approximately equal. A butterfly is composed of column intervals of length $c_i^{wing} = c_i$ containing valid values $H_{ij}^{wing} = H_{ij}$, or of length c^{peak} (i.e. only in a single column i) with valid values H^{peak}, satisfying

$$c_i^{wing} > c^{peak} \quad \text{and} \quad H_{ij}^{wing} < H^{peak} \tag{1}$$

Values c_i^{wing}, H_{ij}^{wing}, c^{peak}, and H^{peak} depend on the number of pixels in the image in the corresponding noisy line segment.

Since the sum of valid values is approximately identical for every column around a peak, the standard variance σ is selected for measuring the *degree of voting scatter* of each column. The smaller the standard variance is, the *more clustered* the voting is. The butterfly's symmetric point is defined by the minimum σ in all contributing columns.

Selection of the Origin in Image Space. Let M and N be width and height of the image space, respectively. In standard Hough transform, the origin in image space is selected to be at a corner of the image, identified with the origin of the coordinate system as used for representing image data. In this case, the range of ρ in the Hough space is from $-\sqrt{M^2+N^2}$ to $\sqrt{M^2+N^2}$, and the range of θ is $[0,\ 180°)$.

If the image centre is selected to be the origin, the range of ρ changes into the interval

$$[-\frac{\sqrt{M^2+N^2}}{2},\ \frac{\sqrt{M^2+N^2}}{2}]$$

Thus, it is reduced to half of its previous size.

The Hough transform equation is then as follows:

$$\rho = (u - \frac{M}{2})\cos\theta + (v - \frac{N}{2})\sin\theta \tag{2}$$

where (u, v) is a pixel coordinate in image space. The location of the origin in the image influences the distance from the perpendicular point P_p to the line segment. By practical experience, this translation of the origin causes a smaller butterfly-like region of valid values of one peak.

Suppose that a line is far away from its perpendicular point; then the butterfly distribution is totally different with respect to either the image corner O or the image centre O'. In case of selecting O as the origin of the image, peak and both wings may not be very distinct in Hough space; several columns may have only one valid cell with the same maxima. The likelihood of such a case is reduced by

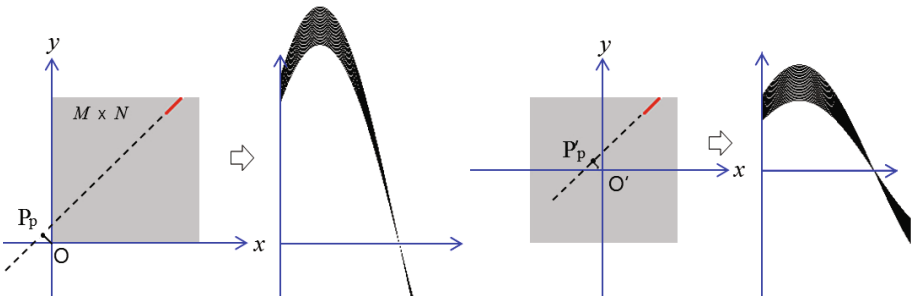

Fig. 3. Butterfly distribution for different coordinate origins. *First and second, from the left*: Image corner as origin, and butterfly in HT space. *Third and fourth*: Same line segment and image centre as origin, and corresponding butterfly in HT space.

selecting O' as the coordinate origin. In general, if O' is the origin, a butterfly region is more distinctly defined by two wings and a symmetrical point.

Figure 3 shows butterfly region distributions for both origin options. In case of the image corner origin, the perpendicular point is far away from the line segment; column interval at the peak has a similar width as column intervals at the ends of the wings in the butterfly region B. It is difficult to detect the peak. In case of the image centre origin, the distance from P_p to line segment is reduced; column intervals in wings of the butterfly are wider, thus defining a more distinct peak.

3 Peak Detection

In this paper, the proposed peak detection procedure combines *finding* of a peak ("roughly") with *localizing* it precisely. After voting for all cells in the accumulator array, the first step is to find a possible peak in the Hough space. Then, for peak localization, accurate peak parameters are estimated by considering peak spreading in the accumulator cells around a found peak.

Peak Finding. The most common method [13] for peak finding is to determine a global threshold first, and to select cells that received more votes than the threshold. Another methods is to identify a peak as a local maxima.

In this paper, a combined local-global method is used for finding an initial peak λ^0, to be accurately localized in the following. The initial peak λ^0 is decided by using the sum of all the nine voting values in a sliding 3×3 window over the whole accumulator array; the window having the maximum sum contains the initial peak λ^0 at its central cell.

Peak Localization. We aim to detect a final peak $\widehat{\lambda}$ as the symmetrical point of the butterfly (identified by λ^0) through our proposed peak localization method which allows us to detect a symmetrical point (as defined above) not only by cell coordinates but even at subcell accuracy (i.e. in real coordinates). The size of a cell is defined by the applied quantization of the Hough space. Our method aims at overcoming the accuracy limitations defined by the quantization setting. Figure 4 illustrates a symmetrical point of a butterfly at subcell accuracy, which identifies a location between adjacent cells, in general with real coordinates.

Let W denote a chosen window, symmetric to λ^0, for approximating the butterfly region B. In our experiments we decided for an 11×11 window W.

We compute the coordinates θ_{peak} and ρ_{peak} of the peak $\widehat{\lambda}$ by using fitting and interpolation techniques. Regarding fitting, we fit a curved function with the σ_i-values for the column intervals in window W; the θ_{peak}-value is defined by the minimum. Regarding interpolation, we compute all m_i-values of the column intervals in window W for computing ρ_{peak} at the obtained θ_{peak}-value.

Statistical means m and variances σ are used as input parameters for those two fitting or interpolation processes. For completeness we provide the basic formulas for the statistical mean m_i and variance σ_i of column intervals symmetric to the

found initial peak λ^0:

$$m_i = \sum_W [H_{ij} \cdot \rho_j] / \sum_W H_{ij} \tag{3}$$

$$\sigma_i = \sqrt{\sum_W [H_{ij} \cdot (\rho_j - m_i)^2] / \sum_W H_{ij}} \tag{4}$$

Window W defines the range of i- and j-values in those sums.

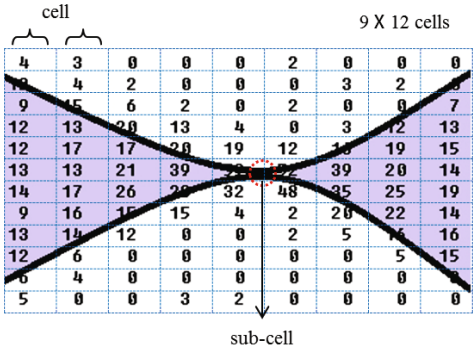

Fig. 4. The symmetric point of a butterfly with subcell accuracy

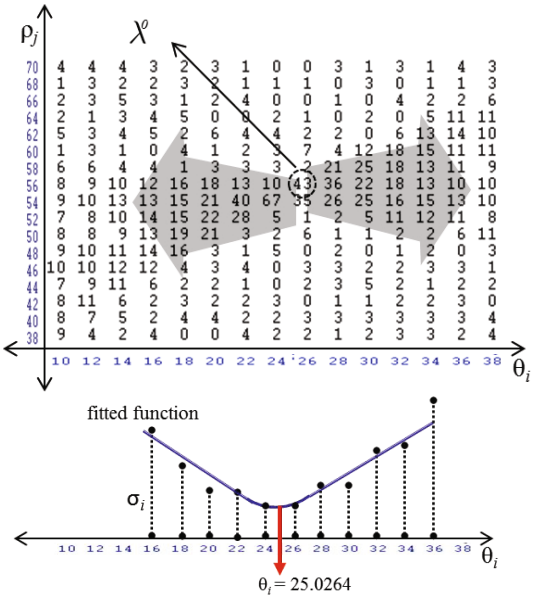

Fig. 5. Function fitting for an 11×11 window W symmetric to the initial peak

Fitting for θ_{peak}. Around λ^0, the localization of the θ-value of the peak is where the voting is "most clustered", as defined by our model in (1).

Since the statistical variance can measure the degree of voting scatter for each θ column, the standard derivation of every column in W, i.e. symmetric to the found peak λ^0, is computed. The θ_{peak}-value at subcell accuracy is computed by fitting a curved function to these standard variances:

1. Compute statistical standard variances σ_i for each column interval left and right of λ^0 within window W.
2. Fit a curved function f with the θ_i and σ_i values:

$$f : \sigma = f(\theta)$$

3. Detect θ_{peak} where this fitted function f has its minima.

$$\theta_{peak} = \theta | f'(\theta) = 0$$

A result is illustrated in Fig. 5. The initial peak λ^0 was found at $(\theta, \rho) = (26, 56)$ with the described peak finding method, and the σ_i-values shown in the bottom part are computed for the shaded cells symmetric to λ^0. A curved function is fitted to those values, the minimum of the function f at $\theta_{peak} = 25.0264$ is of real type, thus not located at a cell but of subcell accuracy.

Interpolation for ρ_{peak}. We calculate the statistical means of θ_i-values in W, i.e. in column intervals left and right of λ^0. The final ρ_{peak} is computed by intersection an interpolated line with the vertical line $\theta_{peak} = 25.0264$:

1. Compute statistical means m_i, for each column interval left and right of λ^0 in window W.

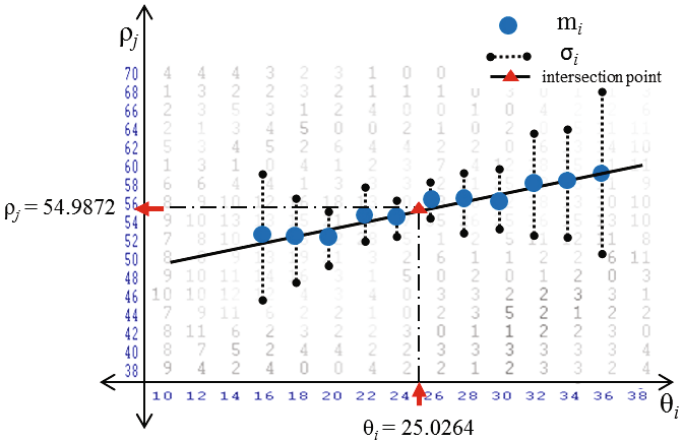

Fig. 6. Linear interpolation for detecting the ρ-value at subcell accuracy

2. Fit a line g with the computed statistical means m_i as follows:

$$g : \rho = g(\theta) \triangleq b_1\theta + b_0$$

3. Compute ρ_{peak} corresponding to the intersection point with the interpolated line:

$$\rho_{peak} = g(\theta_{peak})$$

A result is illustrated in Fig. 6. The computed m_i-values are used for fitting a line, an intersection point is decided then with the defined vertical line at θ_{peak}. The ρ coordinate of the intersection point is the final ρ_{peak}-value. In the shown example, the interpolated ρ_{peak}-value equals 54.9872, and is again a real type for subcell accuracy. The final peak $\widehat{\lambda} = (\theta_{peak}, \rho_{peak})$ is thus detected at $(25.0264, 54.9872)$.

4 Experimental Results

In this section, the proposed peak detection method for the Hough transform is applied at first to a set of simulated data to test the accuracy of line detection. Then we apply the method for real-world data, and selected the detection of lane borders in image sequences recorded for driver assistance purposes.

Test on Simulated Images. We generate $M \times N = 200 \times 200$ binary images that contain 500 randomly generated black pixels as noise. The four endpoint coordinates of one line segment are also produced randomly, and line parameters (θ, ρ) are computed and recorded as ground truth. Black pixels on the line are generated by moving a pixel randomly (i.e. not exactly on the line) by 1 pixel along its normal. A simulated image is shown in Fig. 7, left.

The image centre is selected as the coordinate origin. The accumulator array is quantized by using steps $(\triangle\theta, \triangle\rho) = (2, 2)$. Each pixel votes for all possible cells in the Hough space. After voting, the line parameters are detected with the proposed peak finding and peak localization method. A detection result is shown in Fig. 7, right.

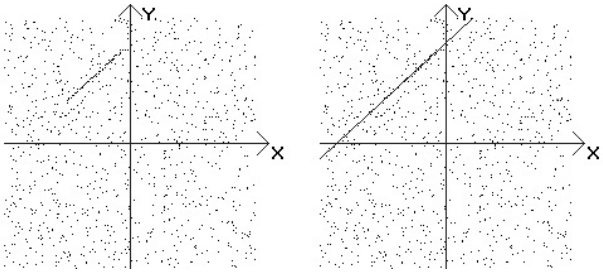

Fig. 7. Line segment detection in simulated images. *Left*: Input image. *Right*: Detected line.

Table 1. Comparison of detection errors

	Detection errors		
	SHT	LSF	F&I
Mean error	(0.633, 0.656)	(0.063, 0.056)	(0.169, 0.119)
Error variance	(0.802, 0.797)	(0.082, 0.075)	(0.210, 0.150)

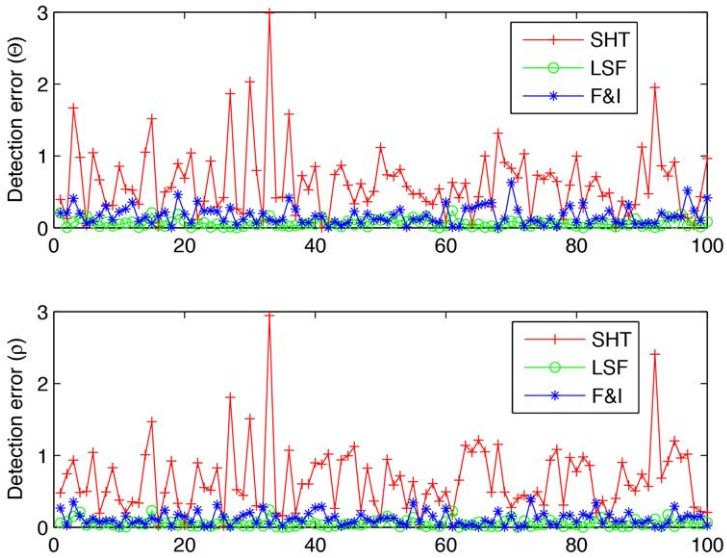

Fig. 8. Comparison of results for 100 generated images

In order to test the detection accuracy, we compare the detection results with the proposed peak localization method (*F&I*) with results obtained either by applying a standard HT (*SHT*), which takes the absolute peak (i.e. with its cell coordinates) as line parameters, or by applying a least-square fit (*LSF*) to the generated line segment pixels, which is regarded as the optimal solution.

For a test for 100 random line segments we report mean error and the error variance. To be precise, the error is measured for both parameters separately, and it is the difference between ground truth value and calculated value. See Table 1. Figure 8 also shows the detection results for the different methods for the 100 input images.

The standard HT is very sensitive to parameter quantization and image noise. Detection errors are larger. By using the fitting and interpolation techniques, we achieve subcell accuracy. By using statistical mean and variance as discussed above, we ensured robustness to image noise. Detection results with the proposed method are actually very close to results obtained by least-square fitting to the

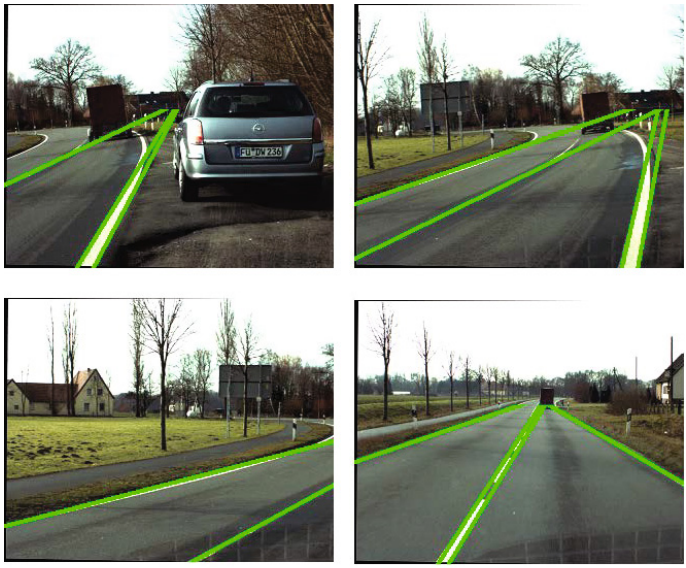

Fig. 9. F&I lane detection results for four frames of real world images

randomly digitized line segments, even under the given coarse quantization and image noise of the reported experiment.

Real World Test. We use image sequences for testing, published in Set 3 of EISATS [6]. These are publicly available long sequences of traffic scenes recorded in Denmark, where lane borders appear to be mostly straight.

One sequence contains 800 frames. When processing these images for line detection, images are first resized to $M \times N = 320 \times 256$, then the image centre is selected as the coordinate origin, and only pixels in the 60% lower part are processed because lane borders are located at the bottom of the whole image. Lane detection results for four images of this data set are shown in Fig. 9.

In a given image, the existence of multiple lines leads to overlays of multiple butterflies in Hough space. We applied multiple-line detection in order to detect accurately every line. The process is as follows: First, a peak $(\theta_{peak}, \rho_{peak})$ is detected by our proposed method, second, a set of pixels contributing to this peak is selected in image space by considering the line parameters and a line thickness, third, the votes of those pixels are removed in accumulator space by decreasing the value in corresponding cells by 1. Then the next peak is found, and so forth until the voting value of the found peak is smaller than a given threshold.

Results show that lane markings are accurately detected if they are "dominantly straight" in the recorded image. With the proposed method, providing

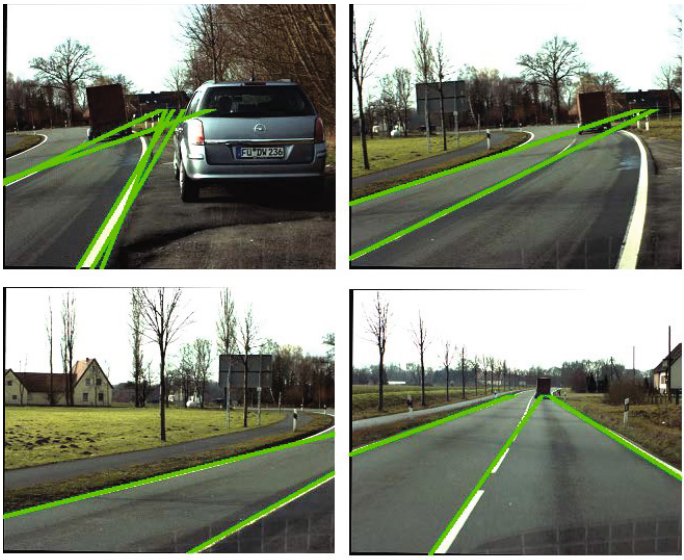

Fig. 10. SHT lane detection results for the same four frames as shown in Fig. 9

subcell accuracy of lane parameters, wide lane markings are identified by two lines (left and right borders).[1]

Lane detection results of the standard HT are also shown in Fig. 10. Some lane borders are missing and there are some spurious lane borders detected. If parameters of a lane border are not matching the used space quantizations then SHT detection results are inaccurate in this case.

5 Conclusions

Peak localization is an important component for any Hough transform procedure. By analysing the butterfly distribution of a peak in Hough space, a statistical mean and variance-based method is proposed to compute accurately the peak parameters. Peak spreading and coordinate origin selection are also considered.

Detection accuracy of the proposed method is compared with that of a standard HT peak detection procedure and an ideal least-squares fitting method. Results show that by fitting and interpolation based on statistical mean and variance, the proposed peak localization method is accurate and robust to parameter quantization and image noise.

[1] An actually operative solution for lane detection could have this as a sub-procedure, combined with temporal reasoning between frames and adaptive curved-line detection at places where straight segments depart from the lane marking in the image. However, we do not aim at presenting a complete lane detection algorithm in this paper; this application is only chosen for illustration of the proposed peak detection technique. For a current review on lane detection methods, see [21].

Acknowledgments. The authors would like to thank Reinhard Klette for his comments and kind support. The first author thanks Jiangsu Overseas Research & Training Program for University Prominent Young & Middle-aged Teachers and President for granting a scholarship to visit and undertake research at The University of Auckland.

References

1. Albanesi, M.G., Ferretti, M., Rizzo, D.: Benchmarking Hough transform architectures for real-time. Real-Time Imaging 6(2), 155–172 (2000)
2. Atiquzzaman, M., Akhtar, M.W.: Complete line segment description using the Hough transform. Image Vision Computation 12(5), 267–273 (1994)
3. Ballard, D.H.: Generalizing the Hough transform to detect arbitrary shapes. Pattern Recognition 13(2), 111–122 (1981)
4. Du, S., Tu, C., van Wyk, B.J., Ochola, E.O., Chen, Z.: Measuring straight line segments using HT butterflies. PLoS ONE 7(3), e33790 (2012)
5. Duda, R.O., Hart, P.E.: Use of the Hough transformation to detect lines and curves in pictures. Comm. ACM 15(1), 11–15 (1972)
6. EISATS:enpeda. image sequence analysis test site (2013), `http://www.mi.auckland.ac.nz/EISATS`
7. Fernandes, L.A.F., Oliveira, M.: Real-time line detection through an improved Hough transform voting scheme. Pattern Recognition 41(1), 299–314 (2008)
8. Furukawa, Y., Shinagawa, Y.: Accurate and robust line segment extraction by analysing distribution around peaks in Hough space. Computer Vision Image Understanding 92(1), 1–25 (2003)
9. Guerreiro, R.F.C., Aguiar, P.M.Q.: Connectivity-enforcing Hough transform for the robust extraction of line segments. IEEE Trans. Image Processing. 21(12), 4819–4829 (2012)
10. Guo, S., Pridmore, T., Kong, Y., Zhang, X.: An improved Hough transform voting scheme utilizing surround suppression. Pattern Recognition Letters 30, 1241–1252 (2009)
11. Hough, P.V.C.: Methods and means for recognizing complex patterns. U.S. Patent 3.069.654 (1962)
12. Illingworth, J., Kittler, J.: The adaptive Hough transform. IEEE Trans. Pattern Analysis Machine Intelligence 9(5), 690–698 (1987)
13. Ji, J., Chen, G., Sun, L.: A novel Hough transform method for line detection by enhancing accumulator array. Pattern Recognition Letters 32(11), 1503–1510 (2011)
14. Kiryati, N., Bruckstein, A.M.: Antialiasing the Hough transform. Graphical Models Image Processing 53, 213–222 (1991)
15. Kiryati, N., Eldar, Y., Bruckstein, A.M.: A probabilistic Hough transform. Pattern Recognition 24(4), 303–316 (1991)
16. Li, H., Lavin, M.A., LeMaster, R.J.: Fast Hough transform: A hierarchical approach. Computer Vision Graphics Image Process 36(2-3), 139–161 (1986)
17. Leavers, V.F., Sandler, M.B.: An efficient Radon transform. In: Int. Conf. Pattern Recognition, pp. 380–389 (1988)
18. Niblack, W., Petkovic, D.: On improving the accuracy of the Hough transform: Theory, simulation, and experiments. In: IEEE Conf. Computer Vision Pattern Recognition, pp. 574–579 (1988)

19. Niblack, W., Petkovic, D.: On improving the accuracy of the Hough transform. Machine Vision Applications 3, 87–106 (1990)
20. Palmer, P.L., Kittler, J., Petrou, M.: An optimizing line finder using a Hough transform algorithm. Computer Vision Image Understanding 67(1), 1–23 (1997)
21. Shin, B.-S., Xu, Z., Klette, R.: Visual lane analysis - a concise review. Technical report MItech-TR-84, The University of Auckland (2013)
22. Tsai, D.M.: An improved generalized Hough transform for the recognition of overlapping objects. Image Vision Computing 15, 877–888 (1997)
23. Tu, C., Du, S., van Wyk, B.J., Djouani, K., Hamam, Y.: High resolution Hough transform based on butterfly self-similarity. Electronics Letters 47(25), 1360–1361 (2011)
24. Xu, L., Oja, E., Kultanen, P.: A new curve detection method: Randomized Hough transform (RHT). Pattern Recognition Letters 11(5), 331–338 (1990)